catalysts

MDPI

Article

Methanol to Gasoline (MTG): Preparation, Characterization and Testing of HZSM-5 Zeolite-Based Catalysts to Be Used in a Fluidized Bed Reactor

Andrés Sanz-Martínez, Javier Lasobras, Jaime Soler *, Javier Herguido and Miguel Menéndez

Catalysis, Molecular Separations and Reactor Engineering Group (CREG), Aragon Institute of Engineering Research (I3A), University of Zaragoza, 50009 Zaragoza, Spain; sanza@unizar.es (A.S.-M.); jlasobra@unizar.es (J.L.); jhergui@unizar.es (J.H.); miguel.menendez@unizar.es (M.M.)
* Correspondence: jsoler@unizar.es; Tel.: +34-876555481

Abstract: The preparation of catalysts suitable for MTG processes in a fluidized bed reactor has been studied with emphasis on improving the textural, physico-chemical, morphological, structural and mechanical properties. A mixture of HZSM-5 zeolite (active material), boehmite or bentonite (binder) and alumina (inert filler) was used to prepare different catalysts. After preparation, characterization by physical adsorption of N_2, XRF, XRD and SEM-EDX techniques was carried out. The screening of catalysts was performed in a fluidized bed reactor. The distribution of products was very similar in all cases, with the yield of light hydrocarbons always being higher than that of gasoline. Among the catalysts tested, the one containing boehmite as a binder (HZ_Boeh) was found as the most appropriate due to its high mechanical strength, high yield to aromatics and lower yield to durene.

Keywords: MTG; HZSM-5; binder; fluidized bed reactor; aromatics; durene

Citation: Sanz-Martínez, A.; Lasobras, J.; Soler, J.; Herguido, J.; Menéndez, M. Methanol to Gasoline (MTG): Preparation, Characterization and Testing of HZSM-5 Zeolite-Based Catalysts to Be Used in a Fluidized Bed Reactor. *Catalysts* **2022**, *12*, 134. https://doi.org/10.3390/catal12020134

Academic Editor: Angelo Vaccari

Received: 22 December 2021
Accepted: 19 January 2022
Published: 22 January 2022

1. Introduction

The MTG (Methanol to Gasoline) process allows us to transform methanol into hydrocarbons within the range of gasoline boiling points [1]. The process emerged in the early 1970s by researchers from ExxonMobil Company. They observed the transformation of a methanol stream into high octane gasoline when using a ZSM-5 type zeolite, which was suitable due to its high specific surface area, acidity and well-defined structure [2].

The conversion of methanol to hydrocarbons can be carried out with a wide variety of acid catalysts. There is literature that reports the use of non-zeolitic catalysts for the MTG reaction [3–5]. However, those based on zeolite are the ones that have offered the best performance. Among them, the HZSM-5 zeolite stands out from the rest [6]. This good behavior is mainly attributed to its internal microporous structure (shape selectivity), constituted by a set of straight and zigzag channels that intersect perpendicularly and that limit:

1. The access of reactants of a kinetic diameter greater than the size of zeolite channels.
2. The formation of compounds of a greater volume than the intersections of the channels (inhibition of reactions with high molecular weight products or polycyclic aromatics).
3. The bulk diffusion of large product molecules.

In addition to shape selectivity, the acidity of zeolite also plays an important role in its catalytic behavior. This is proportional to the aluminum content in its composition. Thus, there are studies that show the influence of the acidity of the catalyst on its activity [7,8] and the dealumination of the zeolite [9].

The process has been simulated in a fixed bed reactor [10] and the mechanisms of reaction [11,12], reaction kinetics [13] and regeneration [14,15] of the catalyst have also been proposed. The following mechanism scheme is commonly assumed [16]:

$$2CH_3OH \rightleftharpoons CH_3OCH_3 + H_2O \quad (1)$$

$$CH_3OCH_3 \rightarrow \text{Light olefins} + H_2O \quad (2)$$

$$\text{Light olefins} + CH_3OCH_3 \rightarrow \text{Heavy olefins} + H_2O \quad (3)$$

$$\text{Heavy olefins} \rightarrow \text{Aromatics} + \text{Paraffins} \quad (4)$$

$$\text{Aromatics} + CH_3OCH_3 \rightarrow \text{Heavy aromatics} + H_2O \quad (5)$$

Although the operation of the HZSM-5 catalyst provides high performance to gasoline, coke is slowly formed on the catalyst and the activity of the catalyst decreases [17]. It has been demonstrated how the use of a fluidized bed reactor (FBR) decreases the amount of coke present on the surface of the catalyst (with respect to a fixed bed). Its mixing regime favors the contact of the catalyst with water vapor generated in the reaction and, consequently, the elimination by stripping of coke [18]. A very common practice in processes that require solids with some mechanical strength (for example, their use in drag or fluidized bed reactors) is the addition of binders. For the MTG process, the binders with the best results are boehmite, bentonite and montmorillonite [6]. However, the use of a binder can alter the zeolite properties by neutralizing the HZSM-5 protons, blocking the zeolite channels during the pelletization process and entrapment by the coke precursor binder [19].

The objective of this work is the preparation, characterization and testing of different catalysts based on HZSM-5 zeolite for the reaction of Methanol to Gasoline (MTG). These present variable percentages of binders (boehmite or bentonite) and inert filler (alumina) to improve their mechanical properties. The catalyst that works best will be tested in the future in a two-zone fluidized bed reactor (TZFBR) that allows the continuous catalyst regeneration in the same container to counteract the catalyst deactivation by coke. This strategy was already successfully implemented for other processes [20–23].

2. Results and Discussion

2.1. Catalyst Characterization

Textural properties of the catalyst and their constituents were examined by N_2 adsorption–desorption analysis (Table 1). In order to find the modifications suffered by the catalysts after the experiments, both the fresh catalysts (before use in reaction), as well as those used, were characterized. It was observed that the BET surface area of the fresh catalysts (210.8–287.9 $m^2 \cdot g^{-1}$) decreased with respect to HZSM-5 zeolite (319.9 $m^2 \cdot g^{-1}$) because the agglomeration process is carried out with species of smaller specific area than the zeolite. It is worth noting that the BET surface area of the catalysts is higher when referring to the theoretical values calculated considering the proportional contribution of its constituents. This could be explained considering that during the mechanical mixing of the components, colloidal alumina particles (or small zeolite crystals) might exert a broadening effect of the binder layered sheets, thus increasing the surface area of the catalyst. This will be checked later by SEM imaging. On the other hand, the large area offered by alpha-alumina (α-Al_2O_3) draws special attention. According to Vieira et al. [24], this alumina phase should not have values greater than 20 $m^2 \cdot g^{-1}$. Subsequently, an XRD analysis was performed, and it was found that the crystalline pattern was more similar to that of the gamma-alumina phase (γ-Al_2O_3).

Table 1. Textural properties of HZSM-5 zeolite, binders (boehmite and bentonite), alumina and prepared catalysts.

Sample	Surface Area [$m^2 \cdot g^{-1}$]		Pore Volume [$cm^3 \cdot g^{-1}$]		Pore Diameter (**) [nm]	
	BET	Micropores (*)	Pores	Micropores (*)	Pores	Micropores
HZSM-5	319.9	202.1	0.23	0.11	2.8	2.2
Boehmite	212.3	-	0.49	-	9.0	-
Bentonite	22.7	4.28	0.083	0.002	14.5	-
Al_2O_3	179.4	-	0.37	-	8.1	-
Fresh catalysts						
HZ_Boeh	287.9	113.4	0.40	0.06	5.5	2.1
HZ_Bent	210.8	57.9	0.35	0.03	6.6	2.1
HZ_Bent+IE	217.6	57.1	0.36	0.03	6.6	2.0
Used catalysts						
HZ_Boeh	271.5	92.5	0.40	0.04	5.8	1.8
HZ_Bent	188.5	49.3	0.35	0.02	7.3	1.8
HZ_Bent+IE	200.6	48.4	0.36	0.021	7.2	1.7

(*) t-plot method; (**) Straight cylindrical pores (4V/A method).

Since the good behavior of HZSM-5 zeolite in the MTG reaction is attributed to the phenomenon of shape selectivity, it is interesting to analyze the microporous properties. Table 1 also shows that the micropore size of the three catalysts and HZSM-5 zeolite remained constant (~2.1 nm). This indicates that the microporous contribution comes uniquely from the zeolite. In addition, the micropore volume of the prepared catalysts, varied proportionally with the HZSM-5 zeolite quantity used in the preparation process (Table 5). The volume of micropores is also preserved after the catalyst preparation process.

Finally, Table 1 shows that the catalysts do not suffer severe textural deterioration after using them in the reaction. There is a slight decrease in its surface area (less than 10%) and in the volume of micropores.

The results of the chemical composition obtained from the XRF characterization are presented in Table 2. The SiO_2/Al_2O_3 molar ratio obtained for the HZSM-5 zeolite was 29.8 (corresponding to the nominal value). The Al_2O_3 percentage of the prepared catalysts increased because of the presence of aluminum in the composition of the inert filler, boehmite and bentonite (montmorillonite type clay). Finally, the sodium content (in the form of Na_2O) in the third catalyst disappeared, which is the signal that the ion exchange treatment took place.

Table 2. Results of X-ray fluorescence analysis (values expressed in wt.%).

Sample	SiO_2	Al_2O_3	Fe_2O_3	MgO	Na_2O	CaO	SO_3	Cl
HZSM-5	94.4	5.4	-	-	-	-	-	-
HZ_Boeh	56.3	43.4	-	-	-	-	-	-
HZ_Bent	44.1	52.8	1.06	0.74	0.45	0.31	0.21	-
HZ_Bent+IE	44.9	52.2	1.09	0.71	-	0.24	0.23	0.27

The XRD technique confirmed the presence of the crystalline phases characteristic of the species that constitute the catalysts, as well as their high crystallinity (good definition of diffractographic peaks).

The morphology and chemical composition of the catalyst constituents were studied using the SEM-EDX technique. Figure 1 shows the appearance of the zeolite HZSM-5 and bentonite.

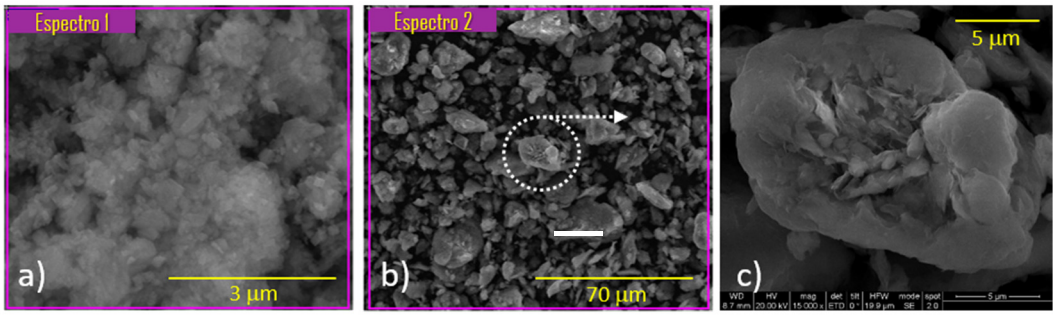

Figure 1. SEM-EDX analysis of different samples: (**a**) the HZSM-5 zeolite, (**b**) the sodium bentonite and (**c**) zoom of the micrograph (**b**) where the laminar shape of the clay is show.

According to EDX analysis (Table 3), the SiO_2/Al_2O_3 molar ratio for the HZSM-5 zeolite was 34.9. This value is analogous to that obtained by XRF for the solid as a bulk (Table 2). This showed that there was no segregation of substances between the bulk and the surface of the particles. Figure 1c shows the laminar structure of the binder. This confirmed the hypothesis stated in the N_2 adsorption–desorption analysis section, where a possible phenomenon of delamination of the binder was established.

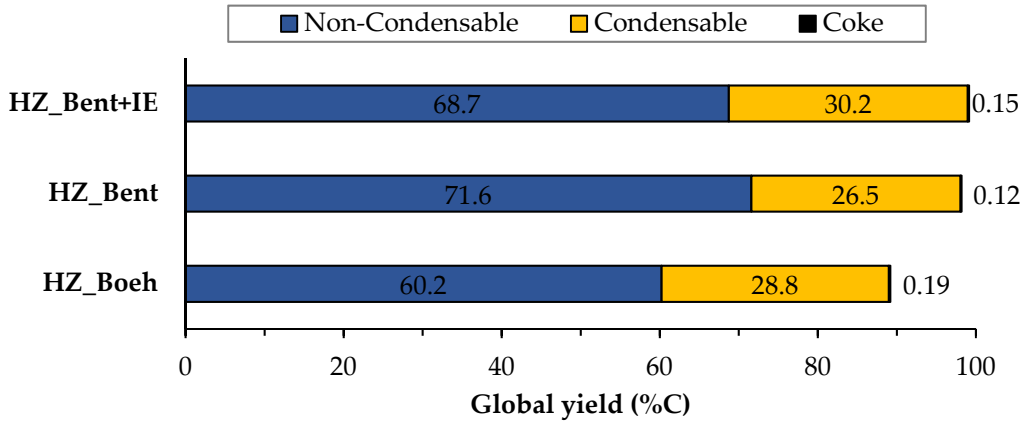

Figure 2. Global distribution of products for the three catalysts. Values calculated as an average of the complete TOS of each experiment. Operating conditions: W/F_{A0} = 11.3 $g_{cat.} \cdot h \cdot mol_{MeOH}^{-1}$; T = 450 °C.

Table 3. Results derived from the EDX analysis for 'Spectrum1' and 'Spectrum 2' of Figure 2 (values expressed in wt.%).

Sample	O	Si	Al	Fe	Mg	Na	Ca
Spectrum 1: HZSM-5	58.2	39.6	2.2	-	-	-	-
Spectrum 2: Bentonite	52.4	29.5	9.6	3.5	1.4	2.5	1.0

2.2. Fluidized Bed Reactor Tests

Figure 2 shows the distribution of products of the three catalysts broken down into gas, liquid and solid (coke) phases, calculated as an average of the complete time on stream (TOS) of each experiment (205 min. for the HZ_Boeh and HZ_Bent+IE catalysts and 220 min. for the HZ_Bent). These phases are obtained, respectively, as: non-condensable fraction (light hydrocarbons), condensable fraction (gasoline) and carbon fraction. Coke deposited in the catalyst during the experiment was calculated from the CO_x gases obtained in its regeneration.

Figures 3 and 4 show the carbon-based yield of the different groups of compounds in the gas and liquid phase, respectively.

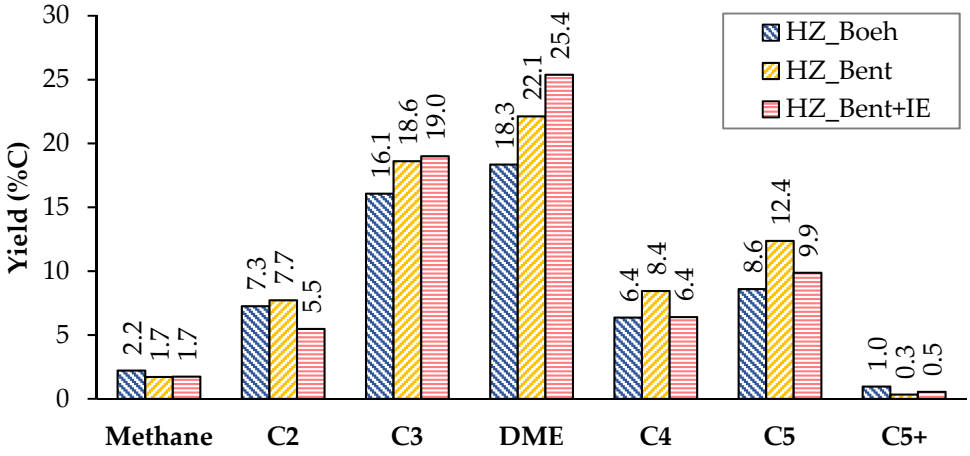

Figure 3. Distribution of products in the gas phase (non-condensable). Values calculated as an average of the complete TOS of each experiment. Operating conditions: W/F_{A0} = 11.3 $g_{cat.} \cdot h \cdot mol_{MeOH}^{-1}$; T = 450 °C.

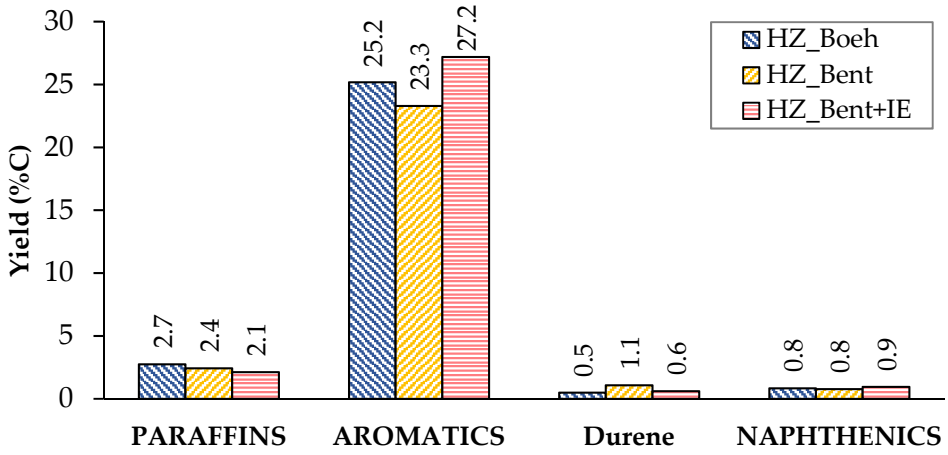

Figure 4. Distribution of products in the liquid phase (condensable). Values calculated as an average of the complete TOS of each experiment. Operating conditions: W/F_{A0} = 11.3 $g_{cat.} \cdot h \cdot mol_{MeOH}^{-1}$; T = 450 °C.

The detailed product distribution, as well as the conversion of methanol and the amount of coke formed, can be seen in Table 4.

There is great similarity in the global distribution of products for the three catalysts. All of them have in common that: (i) the yield to light hydrocarbons is higher than that of gasoline, with a maximum production of these being found with the HZ_Bent+IE catalyst and (ii) the yield to coke is very low. Schulz et al. [25] report the formation of an unstable coke with a low molecular weight and a highly hydrogenated nature. This justifies its possible continuous elimination throughout the reaction by stripping. The HZ_Boeh catalyst has the highest coke formation rate, probably due to its higher zeolitic load (50 wt.%, nominal).

Table 4. Methanol conversion, total carbon fed and carbon-based yield of products for the three catalysts. Operating conditions: W/F_{A0} = 11.3 $g_{cat.} \cdot h \cdot mol_{MeOH}^{-1}$; T = 450 °C.

Catalyst	HZ_Boeh	HZ_Bent	HZ_Bent+IE
MeOH conversion [%]	<99.9	<99.9	<99.9
C total fed [mg]	54,719.7	65,663.7	54,185.9
NON-CONDENSABLE	60.2	71.6	68.7
CH_4	2.2	1.7	1.7
DME	18.3	22.1	25.4
C_2	7.3	7.7	5.5
Ethane	0.4	0.2	0.4
Ethylene	6.9	7.6	5.1
C_3	16.1	18.6	19.0
Propane	6.0	4.8	9.2
Propylene	10.1	13.8	9.8
C_4	6.4	8.4	6.4
C_5	8.6	12.4	9.9
C_5 + (C_6H_6, C_7H_8, . . .)	1.0	0.3	0.5
CO_x	0.4	0.3	0.3
CONDENSABLE	28.8	26.5	30.3
PARAFFINS	2.7	2.4	2.1
2-methyl butane	0.7	0.6	0.6
Pentane	0.3	0.1	0.1
Hexane	0.2	0.1	0.1
C_7 + (alcanes)	0.1	0.1	0.1
AROMATICS	25.2	23.3	27.2
Benzene	1.9	0.6	1.5
Ethylbencene	0.8	0.6	0.7
Toluene	4.3	2.3	3.9
p-Xylene	6.8	6.0	7.8
Durene	0.5	1.1	0.6
NAPHTHENICS	0.8	0.8	0.9
Cyclopentane	0.1	0.0	0.0
Naphthalene	0.0	0.0	0.0
COKE	0.19	0.12	0.15

Considering the distribution of gaseous products, we give a special mention to dimethyl ether (DME). In accordance with Equation (2), DME acts as an intermediate product in the process of transforming methanol to light olefins. In the case of bentonite-based catalysts as binders, the yield to DME increases considerably. An explanation is in a bad fluidization of these solids. The cohesive nature of this binder (bentonite) generated an unwanted fluidization state in which the flow rate went from being continuous to a pulse flow rate. It should be noted that this phenomenon was not observed in previous fluid dynamics tests with nitrogen. This resulted in a shorter residence time for methanol and, more importantly, for intermediates produced in the dehydration of methanol such as DME (due to the fact that for all experiments the W/F_{A0} parameter is high enough to achieve total methanol conversion, even with the possible gas shortcut). Consequently, the yield to DME was higher.

The distribution of liquid products shows a similar yield to the different groups of compounds (paraffins, aromatics and naphthenics) for the three catalysts (Figure 5). Aromatics represent the major contribution, with p-xylene as the most abundant. This high proportion of aromatics is consistent with the characteristics of the gasoline obtained by MTG using zeolitic catalysts. A priori, this should not be a problem, since they are usually species that have a good octane index. On the contrary, durene(1,2,4,5-tetramethylbenzene) is an aromatic hydrocarbon that, due to its high melting point (80 °C), can cause problems of fluidity in gasoline when present in a high concentration. The company Exxon Mobil

determined a limit value of 2% durene in the gasoline for use in vehicles [26]. Among the three catalysts, the lowest yield to durene was obtained with HZ_Boeh (Figure 4).

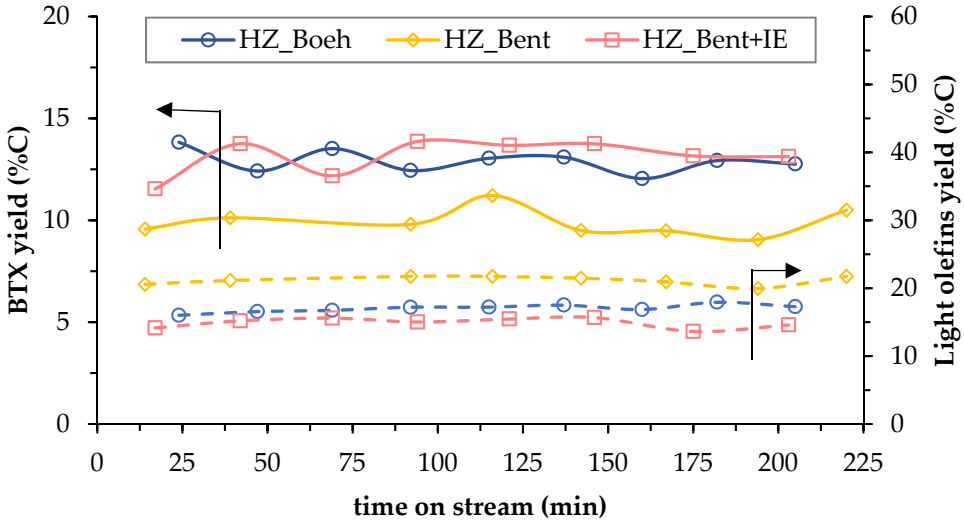

Figure 5. Temporal evolution of carbon-based yield to BTX (solid lines) and light olefins (dashed lines) for the three catalysts.

The stability of the process is analyzed in Figure 5. It shows the effect of TOS on the yield to BTX (which refers to a mixture of benzene, toluene and p-Xylene) and light olefins (ethylene and propylene), both as hydrocarbons more representative of liquid and gaseous products, respectively. There is no clear phenomenon of catalyst deactivation in any of the three cases, since both yields (BTX and light olefins) do not decrease with the TOS (220 min). This effect, together with the low rate of coke formation, concludes that the deactivation of the catalysts, although it may occur, is not appreciable in these experiments (Figure 6) due to the large catalyst mass in the bed (15.1 ± 0.5 g). It should be noted that only the formation of coke has been considered as a cause of deactivation [27].

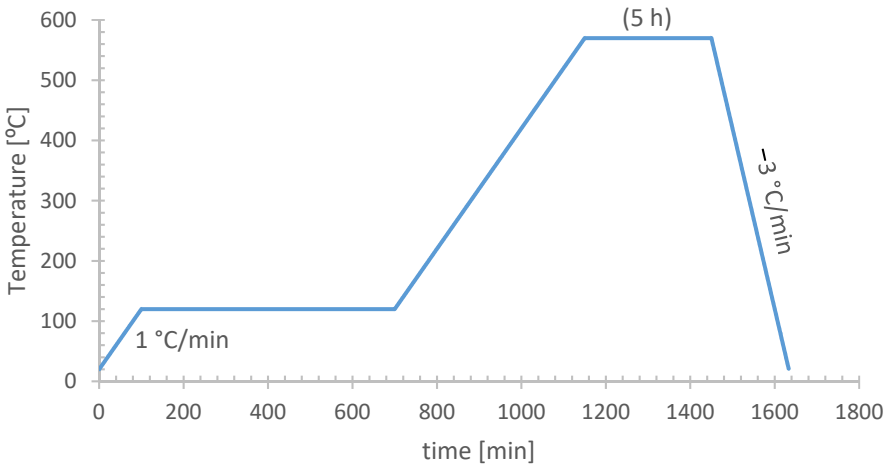

Figure 6. Method for the first calcination of zeolite conditioning: transition from ammonium (NH_4ZSM-5) to proton (HZSM-5) form.

The criteria for selecting the most appropriate catalyst were based on the one with the best fluidization, the lowest yield to durene (limited hydrocarbon in commercial gasolines) and the highest ratio of 'liquid yield versus light hydrocarbons yield'. Thus, the HZ_Boeh catalyst was selected for subsequent experiments using a TZFBR configuration. Although this catalyst showed the highest yield to coke, this is not a problem since in this reactor (TZFBR), the deactivation of the catalyst can be counteracted.

3. Experimental

3.1. Catalyst Preparation

Different catalysts based on the HZSM-5 zeolite (active species) were synthesized in order to select the best behavior in a fluidized bed reactor. Boehmite and bentonite (as binders) and alumina (as inert filler) were used because they increase the resistance to attrition of the catalysts and adapt their particle size for the operation in this type of reactor. Among those catalysts, three of them are selected to analyze the effect of the type and proportion of binder on their performance (Table 5).

Table 5. Composition of the different HZSM-5 zeolite-based catalysts tested (nominal wt.%).

Catalyst	HZSM-5	Boehmite	Bentonite	Al_2O_3	IE (*)	Ref.
	[wt.%]				-	-
HZ_Boeh	50	30	-	20	No	[28]
HZ_Bent	25	-	30	45	No	[29]
HZ_Bent+IE	25	-	30	45	Yes	[30]

(*) Ion exchange (IE) treatment with a 0.6 N solution of HCl.

All catalysts were prepared from commercial ZSM-5 zeolite (molar ratio SiO_2/Al_2O_3 of 30) (CAS No.: 1318-02-1) supplied by Zeolyst International in its ammonium form, boehmite (Sasol Germany, Hamburg, Germany) (CAS No.: 1318-23-6) or bentonite (Sigma Aldrich, St Louis, MO, USA) (CAS n.: 1302-78-9) and an aqueous dispersion of colloidal alumina (Alfa Aesar, Kandel, Germany, 20 wt.%, dp~50 nm) (CAS No.: 1344-28-1).

The preparation procedure of the selected three catalysts can be summarized in two general stages. First, the zeolite in its ammonium form (NH_4ZSM-5) was calcined in a muffle furnace (Nabertherm B180, Lilienthal, Germany) following the Süd-Chemie method (Figure 6). This allowed the zeolite to be converted to its protonic form (HZSM-5), which is catalytically active in the MTG process.

Second, a mixture containing the zeolite HZSM-5, binder (boehmite or bentonite), alumina and a variable content of distilled water was vigorously stirred for 2 h at room temperature. After, this mixture was shaped by the wet extrusion method. The extrudates were dried overnight at room temperature and then in an oven at 110 °C. They were grounded and sieved (160–315 μm) and calcined in muffle furnace (575 °C for 2 h, with a heating rate of 1 °C/min) in order to fix the structure of the synthesized catalyst. As a result, the catalysts HZ_Boeh and HZ_Bent were obtained.

For the synthesis of the third catalyst (HZ_Bent+IE), an ion exchange treatment was applied to the catalyst HZ_Bent. This treatment was proposed as a technique for recovering the acid function that the zeolite could have lost in the previous stage, due to the presence of the alkaline cations Na^+ of the bentonite. The ion exchange was carried out using a 0.6N solution of HCl (35 mL solution/g catalyst). The mixture was stirred at room temperature for 2 h, neutralized, filtered under vacuum and dried in an oven at 90 °C overnight. Once dry, it was ground and sieved to the same particle diameter as the previous ones (160–315 μm).

3.2. Catalyst Characterization

The catalysts and their constituents (zeolite HZSM-5, boehmite, bentonite and alumina) were characterized by physical adsorption of N_2 (TriStar 3000 V6.08 A, Micromeritics, Norcross, GA, USA). This characterization technique was used to determine the size, volume, shape and pore size distribution (BJH method) and specific surface area from the adsorption isotherm (BET method). The samples were outgassed under vacuum for 9 h (1 h at 120 °C and 8 h at 200 °C) before the measurements (VacPrep061, Micromeritics, Norcross, GA, USA).

To determine the chemical composition of the different catalysts and the HZSM-5 zeolite, X-ray fluorescence (XRF) was performed (ARL series and ADVANT/XP model, Thermo Electron) with a ray tube Rhodium X. The UNIQUANT program was used for semiquantitative analysis without standards (sequential analysis from Mg to U). In addition, XRF was used to verify whether the ion exchange treatment carried out in the third catalyst took place, that is, the Na^+ cations had been completely replaced.

The crystalline structures of the catalysts, the binders and the HZSM-5 zeolite were determined by X-Ray diffraction (XRD) with a Panalytical Empyrean diffractometer, equipped with a Cu anode and a monochromator to select the CuKα radiation (λ = 1.5418 Å). The 2θ angle range was covered from 10 to 90° (step of 0.013° and speed of 2.6 s per step). For the analysis of diffractograms, HighScore software was used.

Scanning electron microscopy (SEM) was performed to analyze the surface roughness and grain size. SEM was applied to the second catalyst (HZ_Bent), the HZSM-5 zeolite and bentonite. The equipment used is an INSPECT-F50 of the FEI Company. This equipment generates an electric field with potential differences between 1 and 30 kV. This technique has also been used to find the chemical composition by EDX analysis of the samples.

3.3. Fluidized Bed Reactor Tests

The reaction system was based in a quartz-made cylindrical fluidized bed reactor (FBR), with a 27 mm internal diameter and 300 mm in height. The reactor was operated at atmospheric pressure and placed inside an electrical furnace at 450 °C. Temperature was monitored by means of a K-type thermocouple (at the center of the catalyst bed) connected to a PID control (Controller 3116, Eurotherm, West Sussex, U.K.). A porous quartz plate with pores smaller than 90 μm supported the catalyst bed (15 g) and acted as the gas distributor. Liquid methanol (90 vol.%) was fed by an HPLC pump (Shimadzu LC-10AT VP, Suzhou, China). After passing through an evaporator (250 °C), it was conducted to the reactor by means of a carrier gas (N_2). Gases were fed using mass flow controllers (Alicat Scientific, Tucson, AZ, USA). The gas stream of products was passed through a condensation unit (−6 °C) at atmospheric pressure. The non-condensable fraction (permanent gases and light hydrocarbons) was quantified using a bubble flowmeter and analyzed by gas chromatography (Varian CP3800, with TCD and FID detectors, Walnut Creek, CA, USA). The analysis of the condensable fraction (gasoline, water and possible traces of unreacted methanol) was performed in discrete samples (1 μL) by means of gas chromatography-mass spectrometry (Shimadzu GCMS-QP2010, Canby, OR, USA). The frequency of analysis, both gases and liquids, was 22 min.

In all cases, the feeding was carried out through the lower part of the reactor (conventional fluidized bed). The superficial velocity of the fed gas (u_0) was twice the minimum fluidization velocity (u_{mf}) and space time (W/F_{A0}) was kept at a value of 11.3 $g_{cat.}\cdot h\cdot mol_{MeOH}{}^{-1}$. After the reaction step, it was necessary to regenerate the catalyst by combustion of coke. All regenerations were carried out at 550 °C with a total flow of 250 $STPmL\cdot min^{-1}$ and 2 vol.% O_2 composition (N_2 balance). Table 6 shows a summary of the main operating conditions.

Table 6. Experimental conditions of fluidized bed reactor experiments.

Temperature	Catalyst Weight	u_r (u_0/u_{mf})	MeOH Feed	W/F_{A0}
[°C]	[g]	-	[vol.%]	[$g_{cat.}\cdot h\cdot mol_{MeOH}{}^{-1}$]
450	15.1 ± 0.5	2	90	11.3

All regenerations: 550 °C and 250 $STPmL\cdot min^{-1}$ (2 vol.% O_2).

4. Conclusions

Three catalysts suitable for use in a fluidized bed reactor (FBR) in the MTG process were prepared, characterized and tested. These were based on HZSM-5 zeolite (as active phase) and different proportions of a binder (boehmite and bentonite) and inert filler

(alumina). The catalysts showed high specific surfaces with 211 $m^2 \cdot g^{-1}$ in the worst case (non-ion-exchange bentonite catalyst). In addition, the microporous and crystalline internal structure of the zeolite HZSM-5 was preserved after the synthesis process. They were active in reaction and did not suffer a severe textural deterioration after use (decrease of approximately 10% in their specific areas).

The catalyst containing boehmite as a binder, with the composition of 50 wt.% HZSM-5, 30 wt.% boehmite and 20 wt.% alumina, was selected as the most suitable catalyst. This one showed the highest ratio of liquids versus gases, did not have the fluidization problems found with bentonite catalysts and had the lowest selectivity to durene. In addition, its coke formation rate was acceptable for future use in a two-zone fluidized bed reactor (TZFBR).

Author Contributions: Conceptualization, J.S., J.H. and M.M.; methodology, J.S., J.H. and M.M.; validation, A.S.-M. and J.L.; writing—original draft preparation, J.S. and J.H.; supervision, M.M. All authors have read and agreed to the published version of the manuscript.

Funding: This publication is part of the projects CTQ2016-76533-R and PID2019-106196RB-I00 supported by MCIN/AEI/10.13039/501100011033.

Data Availability Statement: The study did not report any data.

Conflicts of Interest: The authors declare no conflict of interest.

References

1. Zaidi, H.A.; Pant, K.K. Catalytic conversion of methanol to gasoline range hydrocarbons. *Catal. Today* **2004**, *96*, 155–160. [CrossRef]
2. Kuo, J.C.W. Conversion of Methanol to Gasoline Components. US Patent 3931349, 6 January 1976.
3. Kim, L.; Wald, M.M.; Brandenberger, S.G. One-step catalytic synthesis of 2,2,3-trimethylbutane from methanol. *J. Org. Chem.* **1978**, *43*, 3432–3433. [CrossRef]
4. Hayashi, H.; Moffat, J.B. Conversion of methanol into hydrocarbons over ammonium 12-tungstophosphate. *J. Catal.* **1983**, *83*, 192–204. [CrossRef]
5. Misono, M. Heterogeneous Catalysis by Heteropoly Compounds of Molybdenum and Tungsten. *Catal. Rev. Sci. Eng.* **1987**, *29*, 269–321. [CrossRef]
6. Galadima, A.; Muraza, O. From synthesis gas production to methanol synthesis and potential upgrade to gasoline range hydrocarbons: A review. *J. Nat. Gas Sci. Eng.* **2015**, *25*, 303–316. [CrossRef]
7. Gayubo, A.G.; Benito, P.L.; Aguayo, A.T.; Olazar, M.; Bilbao, J. Relationship Between Surface-Acidity and Activity of Catalysts in the Transformation of Methanol into Hydrocarbons. *J. Chem. Tech. Biotechnol.* **1996**, *65*, 186–192. [CrossRef]
8. Fathi, S.; Sohrabi, M.; Falamaki, C. Improvement of HZSM-5 performance by alkaline treatments: Comparative catalytic study in the MTG reactions. *Fuel* **2014**, *116*, 529–537. [CrossRef]
9. Campbell, S.M.; Bibby, D.M.; Coddington, J.M.; Howe, R.F. Dealumination of HZSM-5 Zeolites II. Methanol to Gasoline Conversion. *J. Catal.* **1996**, *161*, 350–358. [CrossRef]
10. Aguayo, A.T.; Gayubo, A.G.; Castilla, M.; Arandes, J.M.; Olazar, M.; Bilbao, J. MTG Process in a Fixed-Bed Reactor. Operation and Simulation of a Pseudoadiabatic Experimental Unit. *Ind. Eng. Chem. Res.* **2001**, *40*, 6087–6098. [CrossRef]
11. Tajima, N.; Tsuneda, T.; Toyama, F.; Hirao, K. A New Mechanism for the First Carbon−Carbon Bond Formation in the MTG Process: A Theoretical Study. *J. Am. Chem. Soc.* **1998**, *120*, 8222–8229. [CrossRef]
12. Haw, J.F.; Song, W.; Marcus, D.M. The mechanism of methanol to hydrocarbon catalysis. *Acc. Chem. Res.* **2003**, *36*, 317–326. [CrossRef]
13. Benito, P.L.; Gayubo, A.G.; Aguayo, A.T.; Castilla, M.; Bilbao, J. Concentration-Dependent Kinetic Model for Catalyst Deactivation in the MTG Process. *Ind. Eng. Chem. Res.* **1996**, *35*, 81–89. [CrossRef]
14. Janssens, T.V.W. A new approach to the modeling of deactivation in the conversion of methanol on zeolite catalysts. *J. Catal.* **2009**, *264*, 130–137. [CrossRef]
15. Schulz, H. "Coking" of zeolites during methanol conversion: Basic reactions of the MTO-, MTP- and MTG processes. *Catal. Today* **2010**, *154*, 183–194. [CrossRef]
16. Sun, X.; Mueller, S.; Liu, Y.; Shi, H.; Haller, G.L.; Sanchez-Sanchez, M.; van Veen, A.C.; Lercher, J.A. On reaction pathways in the conversion of methanol to hydrocarbons on HZSM-5. *J. Catal.* **2014**, *317*, 185–197. [CrossRef]
17. Lee, S.; Choi, M. Unveiling coke formation mechanism in MFI zeolites during methanol-to-hydrocarbons conversion. *J. Catal.* **2019**, *375*, 183–192. [CrossRef]
18. Aguayo, A.T.; Gayubo, A.G.; Ortega, J.M.; Olazar, M.; Bilbao, J. Catalyst deactivation by coking in the MTG process in fixed and fluidized bed reactors. *Catal. Today* **1997**, *37*, 239–248. [CrossRef]

19. Lasobras, J.; Medrano, J.A.; Soler, J.; Herguido, J.; Menéndez, M.; Jimenez Da Silva, M.; Franco, M.J.; Barrio, I.; Lázaro, J. Preparation of Mo/HZSM-5/Bentonite Catalyst for Methane Aromatization in a Fluidized Bed Reactor. *Int. J. Chem. Reactor Eng.* **2017**, *81*, 1–9. [CrossRef]
20. Herguido, J.; Menéndez, M.; Santamaría, J. On the use of fluidized bed catalytic reactors where reduction and oxidation zones are present simultaneously. *Catal. Today* **2005**, *100*, 181–189. [CrossRef]
21. Pérez-Moreno, L.; Soler, J.; Herguido, J.; Menéndez, M. Stable hydrogen production by methane steam reforming in a two-zone fluidized-bed reactor: Effect of the operating variables. *Int. J. Hydrog. Energy* **2013**, *38*, 7830–7838. [CrossRef]
22. Herguido, J.; Menéndez, M. Advances and trends in two-zone fluidized-bed reactors. *Curr. Opin. Chem. Eng.* **2017**, *17*, 15–21. [CrossRef]
23. Zambrano, D.; Soler, J.; Herguido, J.; Menéndez, M. Kinetic Study of Dry Reforming of Methane Over Ni–Ce/Al_2O_3 Catalyst with Deactivation. *Top. Catal* **2019**, *62*, 456–466. [CrossRef]
24. Vieira Coelho, A.C.; Rocha, G.A.; Souza Santos, P.; Souza Santos, H.; Kiyohara, P.K. Specific surface area and structures of aluminas from fibrillary pseudoboehmite. *Matéria* **2008**, *13*, 329–341. [CrossRef]
25. Schulz, H.; Lau, K.; Claeys, M. Kinetic regimes of zeolite deactivation and reanimation. *Appl. Catal. A Gen.* **1995**, *132*, 29–40. [CrossRef]
26. Fitch, F.; Lee, W. Methanol-to-Gasoline, An Alternative Route to High Quality Gasoline. *SAE Trans.* **1981**, *90*, 4193–4207.
27. Benito, P.L.; Aguayo, T.; Gayubo, A.G.; Bilbao, J. Catalyst Equilibration for Transformation of Methanol into Hydrocarbons by Reaction−Regeneration Cycles. *Ind. Eng. Chem. Res.* **2016**, *35*, 2177–2182. [CrossRef]
28. Pérez-Uriarte, P.; Ateka, A.; Gamero, M.; Aguayo, A.T.; Bilbao, J. Effect of the Acidity of HZSM-5 Zeolite and the Binder in the DME Transformation to Olefins. *Ind. Eng. Chem. Res.* **2016**, *35*, 81–89. [CrossRef]
29. Pérez-Uriarte, P.; Gamero, M.; Ateka, A.; Díaz, M.; Aguayo, A.T.; Bilbao, J. Effect of the Operating Conditions in the Transformation of DME to olefins over a HZSM-5 Zeolite Catalyst. *Ind. Eng. Chem. Res.* **2016**, *55*, 6569–6578. [CrossRef]
30. Cañizares, P.; Durán, A.; Dorado, F.; Carmona, M. The role of sodium montmorillonite on bounded zeolite-type catalysts. *Appl. Clay Sci.* **2000**, *16*, 273–287. [CrossRef]